Ultrafast Dynamics of Photochemical Radical Formation from [Re(R)(CO)$_3$(dmb)] (R = Me, Et; dmb = 4,4′-dimethyl-2,2′-bipyridine): A Femtosecond Time-Resolved Visible Absorption Study

Ian R. Farrell,[a] Pavel Matousek,[b] Cornelis J. Kleverlaan,[c] and Antonín Vlček, Jr.*[a]

Abstract: The excited-state dynamics and photochemistry of [Re(R)(CO)$_3$(dmb)] (R = Me, Et; dmb = 4,4′-dimethyl-2,2′-bipyridine) in CH_2Cl_2 have been studied by time-resolved visible absorption spectroscopy on a broad time scale ranging from approximately 400 fs to a few microseconds, with emphasis on the femtosecond and picosecond dynamics. It was found that the optically prepared Franck–Condon ^{1}MLCT (singlet metal-to-ligand charge transfer) excited state of [Re(R)(CO)$_3$(dmb)] undergoes femtosecond branching between two pathways ($\leqslant$ 400 fs for R = Me; approximately 800 fs for R = Et). For both methyl and ethyl complexes, evolution along one pathway leads to homolysis of the Re–R bond via a ^{3}SBLCT (triplet σ-bond-to-ligand charge transfer) excited state, from which [Re(S)(CO)$_3$(dmb)]$^\cdot$ and R$^\cdot$ radicals are formed. The other pathway leads to an inherently unreactive ^{3}MLCT state. For [Re(Me)(CO)$_3$(dmb)], the ^{3}MLCT state lies lowest in energy and decays exclusively to the ground state with a lifetime of approximately 35 ns, thereby acting as an excitation energy trap. The reactive ^{3}SBLCT state is higher in energy. The quantum yield (0.4 at 293 K) of the radical formation is determined by the branching ratio between the two pathways. [Re(Et)(CO)$_3$(dmb)] behaves differently: branching of the Franck–Condon state between two pathways still occurs, but the ^{3}MLCT excited state lies above the dissociative ^{3}SBLCT state and can decay into it. This shortens the ^{3}MLCT lifetime to 213 ps in CH_2Cl_2 or 83 ps in CH_3CN. Once populated, the ^{3}SBLCT state evolves toward radical photoproducts [Re(S)(CO)$_3$(dmb)]$^\cdot$ and Et$^\cdot$. Thus, population of the ^{3}MLCT excited state of [Re(Et)(CO)$_3$(dmb)] provides a second, delayed pathway to homolysis. Hence, the quantum yield is unity. The photochemistry and excited-state dynamics of [Re(R)(CO)$_3$(dmb)] (R = Me, Et) complexes are explained in terms of the relative ordering of the Franck–Condon, ^{3}MLCT, and ^{3}SBLCT states in the region of vertical excitation and along the Re–R reaction coordinate. A qualitative potential energy diagram is proposed.

Keywords: dynamics · homolytic cleavage · organometallic compounds · photochemistry · rhenium

Introduction

Photochemical homolysis of metal–alkyl bonds is a newly recognized[1–12] but typical reaction of organometallic alkyl–diimine complexes, observed for compounds of the type [M(R)(CO)$_3$(α-diimine)] (M = Mn, Re), [Ru(R)(E)(CO)$_2$(α-diimine)], [Pt(CH$_3$)$_4$(α-diimine)], or main group species such as [Zn(CH$_3$)$_2$(α-diimine)]. Similar photochemistry, involving homolysis of a metal–metal bond, occurs for analogous bimetallic complexes[1–3, 13] [Re(ML$_n$)(CO)$_3$(α-diimine)] or [Ru(ML$_n$)(E)(CO)$_2$(α-diimine)] (ML$_n$ = Ph$_3$Sn, Mn,Re(CO)$_5$), or even for diimine-substituted clusters[14, 15] such as [Os$_3$(CO)$_{10}$(α-diimine)]. Notably, organometallic alkyl–diimines are strongly colored and undergo bond homolysis on irradiation into their lowest absorption band. These reactions thus represent a unique way of efficiently generating reactive radicals using low-energy visible light, with possible applications in photoinitiation.

The photochemistry and photophysics of diimine complexes are generally believed to originate in low-lying $d_\pi \rightarrow \pi^*$, metal-to-ligand charge transfer (MLCT) excited states. However, σ-bond-to-ligand charge transfer (SBLCT or $\sigma\pi^*$) excited states were recently identified[1–3, 5–7, 10, 11, 16–21] as being

[a] A. Vlček, Jr., I. R. Farrell
Department of Chemistry, Queen Mary and Westfield College (University of London)
London E1 4NS (UK)
Fax: (+44) 20-7882-7794
E-mail: a.vlcek@qmw.ac.uk

[b] P. Matousek
Central Laser Facility, CLRC Rutherford Appleton Laboratory
Chilton, Didcot, Oxfordshire OX11 0QX (UK)

[c] C. J. Kleverlaan
Anorganisch Chemisch Laboratorium
Institute of Molecular Chemistry
Universiteit van Amsterdam, Nieuwe Achtergracht 166
1018 WV Amsterdam (The Netherlands)

  0947-6539/00/0608-1386 $ 17.50+.50/0 *Chem. Eur. J.* **2000**, *6*, No. 8

responsible for the photochemical homolysis of metal–ligand bonds observed in these compounds. SBLCT states are introduced to diimine complexes by ligands such as alkyl groups or metal fragments, which are covalently bound to the metal atom by a high-lying σ orbital.[1–3] The SBLCT state, then, originates in electron excitation from a metal–alkyl σ-bonding orbital into a π^* orbital of an electron-accepting α-diimine ligand. Generally, an SBLCT state has the same symmetry and occurs in the same energy range as some $d_\pi \rightarrow \pi^*$ MLCT states. Hence, extensive mixing between MLCT and SBLCT characters can occur, both in the optically prepared Franck–Condon state and in the reactive state proper.[20–22] The extent of this mixing depends on the nature of the ligands and the metal. Quantum chemical calculations have suggested that the changing interactions between SBLCT and MLCT states along possible reaction coordinates can give rise to energy barriers and affect strongly the initial excited-state dynamics and resulting photochemistry.[17, 18, 20, 21] Moreover, the triplet spin multiplicity of the reactive SBLCT excited state, predicted by theoretical considerations,[18, 20, 21] has been firmly established by nanosecond time-resolved FT-EPR studies of [Re(R)(CO)$_3$(α-diimine)] and [Ru(R)(I)-(CO)$_2$(α-diimine)] complexes.[8, 23, 24]

The photochemistry of the [Re(R)(CO)$_3$(α-diimine)] complexes (Figure 1) shows a remarkable dependence on molecular structure and medium; they are excellent examples for

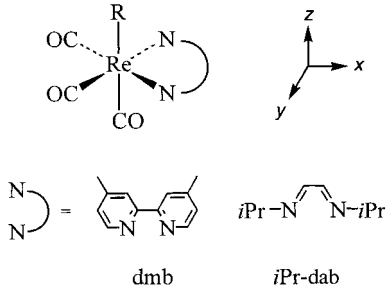

Figure 1. Structure of the *fac*-[Re(R)(CO)$_3$(α-diimine)] complexes and the 4,4′-dimethyl-2,2′-bipyridine (dmb) and *N,N′*-bis(isopropyl)-1,4-diaza-1,3-butadiene (*i*Pr-dab) ligands.

mechanistic studies. The quantum yield, reaction rate, and mechanism of the Re–alkyl bond homolysis [Eq. (1); S = solvent] depend dramatically on the chemical nature of the

$$[Re(R)(CO)_3(\alpha\text{-diimine})] \xrightarrow{h\nu,\,S} [Re(S)(CO)_3(\alpha\text{-diimine})]^{\cdot} + R^{\cdot} \qquad (1)$$

alkyl and α-diimine ligands, and the solvent.[1–3, 6–8] Previous studies[5–8] have indicated that the rate of Re–Me bond homolysis is very fast, presumably sub-picosecond, for all the [Re(Me)(CO)$_3$(α-diimine)] complexes investigated so far. However, quantum yields are relatively low and strongly dependent on the diimine ligand, on temperature, and in some cases[7] on irradiation wavelength. This is due to a concurrent population of low-lying trapping states.[7, 8] Yet quantum yields measured for the ethyl, isopropyl, or benzyl complexes approach unity and are (nearly) independent of temperature.[7, 8] The nature of the diimine ligand influences strongly the rate of the Re–R (R = Et, *i*Pr, Bz) bond homolysis, which is very fast ($\ll$ 7 ns) for complexes containing the aromatic diimine ligand 4,4′-dimethyl-2,2′-bipyridine (dmb), but rather slow (60–250 ns) for *i*Pr–dab complexes (dab = 1,4-diaza-1,3-butadiene), at least in hydrocarbon solvents.[7, 8] A spectacular acceleration (at least 10^5-fold) of the homolysis rate was found for [Re(R)(CO)$_3$(*i*Pr-dab)] (R = Et, Bz) on changing to polar or coordinating solvents.[7]

An understanding of the mechanism of photochemical metal–alkyl bond homolysis in alkyl–diimine complexes can help to answer some fundamental questions of organometallic photochemistry. It can shed light on the marked dependence of the rates and quantum yields on structure and medium, and develop our understanding of the relationships between molecular structure, the nature of the optically prepared and reactive excited states, and the outcome of photochemical reactions. Interaction between MLCT and SBLCT excited states is another interesting point which becomes especially important for Re complexes.[20–22, 25] Up until now, the photochemistry of alkyl–diimine complexes has not been studied on the ultrafast time scale, even though it is the initial excited-state dynamics that are expected to determine the overall course and mechanism of metal–alkyl bond homolysis. Hence, we have investigated the photochemistry of [Re-(Me)(CO)$_3$(dmb)] and [Re(Et)(CO)$_3$(dmb)] in the femto-second–picosecond time domain by time-resolved absorption spectroscopy in the visible spectral region. The remarkable differences in photochemical reactivity between these two complexes were found to reflect different excited-state dynamics ensuing from the optical excitation. The conclusions from this study are applicable to a wide range of organo-metallic photochemical reactions.

Results and Discussion

Absorption spectra: The [Re(R)(CO)$_3$(dmb)] (R = Me, Et) complexes show a well-developed, intense [$\varepsilon = (2.5-3.0) \times 10^3\,\text{M}^{-1}\,\text{cm}^{-1}$] absorption band in the visible spectral region. In CH_2Cl_2, it occurs at $\lambda_{max} = 415$ nm (Me) and 425 nm (Et). In CH_3CN, it is slightly blue-shifted to 400 and 406 nm, respectively.[26] On the basis of solvatochromism and resonance Raman spectra measured for [Re(Me)(CO)$_3$(dmb)], this band was assigned to the lowest allowed $d_{xz} \rightarrow \pi^*$(bpy) MLCT transition.[4, 8, 26] However, recent CASSCF calculations on [Mn(R)(CO)$_3$(H-dab)] and [Re(H)(CO)$_3$(H-dab)] suggest[20–22; 27] that significant mixing of characters occurs between $d_{xz} \rightarrow \pi^*$ MLCT and $\sigma \rightarrow \pi^*$ SBLCT excitations in this transition. Nevertheless, for simplicity, the Franck–Condon excited state is denoted here as ^{1}MLCT. Similarly, other relevant excited states are abbreviated to MLCT or SBLCT, according to their respective predominant character at the geometry of vertical excitation. It should be noted that, even here, strong mixing between MLCT and SBLCT characters occurs, the extent of which generally changes along the Re–R coordinate.[18, 21, 22, 27, 28]

Photochemistry and quantum yields: Previous studies[4, 8, 26] have shown that irradiation of [Re(R)(CO)$_3$(dmb)] (R = Me, Et) in toluene, THF or CH_2Cl_2 produces [Re(S)(CO)$_3$(dmb)]$^{\cdot}$ radicals according to Equation (1). These radicals were detected[26] by EPR spectroscopy, either directly or as adducts

with nitrosodurene or PPh_3. The alkyl radicals ($Me^{\bullet}$ or $Et^{\bullet}$) were observed[8, 23, 24] by FT-EPR in toluene or 2-propanol solutions. Irradiation of $[Re(R)(CO)_3(dmb)]$ at wavelengths above 420 nm in CH_2Cl_2 affords $[Re(Cl)(CO)_3(dmb)]$ (regardless of R), by reaction of the photoproduced $[Re(S)(CO)_3(dmb)]^{\bullet}$ radicals with the CH_2Cl_2 solvent. UV/Vis, IR, and ^1H NMR spectra monitored in the course of the reaction have demonstrated that it proceeds as a clean conversion, $[Re(Cl)(CO)_3(dmb)]$ being the only rhenium-containing product. Quantum yields were determined in CH_2Cl_2 with a 488 nm Ar^+ laser line as the irradiation source. Conversion was kept below 5%. UV/Vis spectra monitored during quantum yield measurements showed a well developed isosbestic point. No signs of any side reaction or decomposition have been noticed. A striking difference in behavior was found between the Me and Et complexes. The quantum yield of the Re–Me bond homolysis in $[Re(Me)(CO)_3(dmb)]$ is temperature-dependent; a value of 0.4 was determined at 293 K.[8, 26] However, a temperature-independent quantum yield of approximately 1 was measured for $[Re(Et)(CO)_3(dmb)]$, in accordance with previous results.[26] Quantum yields from toluene solutions[8] are very close to those found from CH_2Cl_2.

Nanosecond time-resolved absorption spectra recorded in toluene have been investigated in great detail.[8] We found qualitatively identical nanosecond kinetics for solutions in CH_2Cl_2, the solvent used in our ultrafast studies. Corresponding nanosecond absorption spectra are shown in Figures 2 and 3,

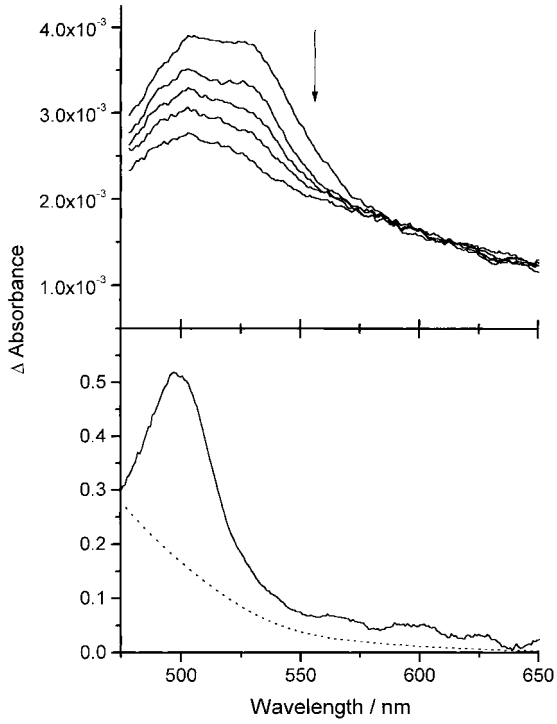

Figure 2. Transient difference absorption spectra of $[Re(Et)(CO)_3(dmb)]$ in CH_2Cl_2. Top: spectra measured at time delays of 5, 50, 100, 200, and 700 ps, respectively, in the direction of the arrow, after 400 nm, 250 fs FWHM excitation, with a magic angle orientation of the polarization directions of the excitation and probe pulses. Bottom: nanosecond spectrum measured at 10 ns after 355 nm, 7 ns FWHM excitation. Dotted curve, ground-state absorption spectrum.

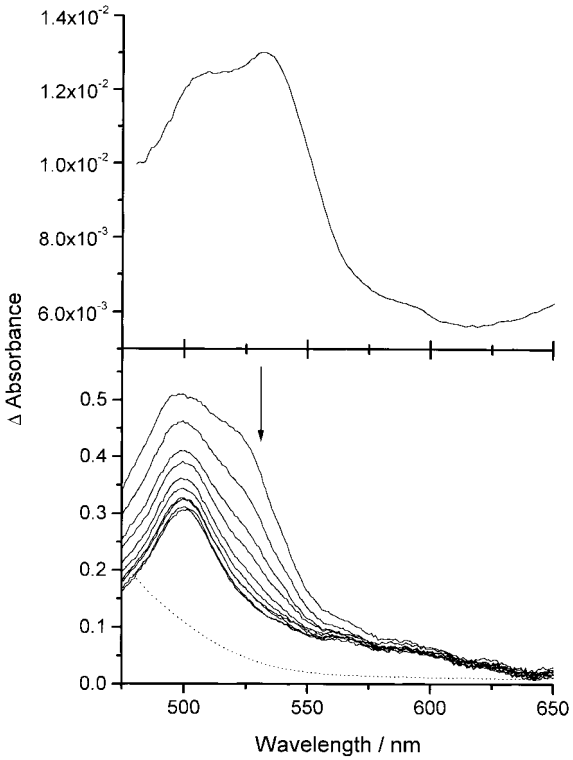

Figure 3. Transient difference absorption spectra of $[Re(Me)(CO)_3(dmb)]$ in CH_2Cl_2. Top: spectrum measured at 5 ps after 400 nm, 250 fs FWHM excitation, with a magic angle orientation of the polarization directions of the excitation and probe pulses. Bottom: nanosecond spectra measured after 355 nm, 7 ns FWHM excitation. First spectrum at 10 ns; interval between following measurements 10 ns. Dotted curve, ground-state absorption spectrum.

bottom panel. Excitation of $[Re(Et)(CO)_3(dmb)]$ produces a long-lived transient with an absorption maximum at approximately 500 nm (Figure 2), while a weak, unresolved absorption extends over the whole visible region above 800 nm. This transient spectrum is characteristic[4, 8] of the $[Re(S)(CO)_3(dmb)]^{\bullet}$ radical. This assignment was based[8] on an independent identification of $[Re(S)(CO)_3(dmb)]^{\bullet}$ as the primary photoproduct by time-resolved IR (TRIR)[8] and EPR spectroscopy[8, 26] and on comparison with the absorption spectrum of $[Re(Cl)(CO)_3(dmb)]^{\bullet-}$, which (at 198 K) shows a strong absorption band at 512 nm with a shoulder at 483 nm.[29] Moreover, nanosecond laser flash photolysis of several complexes $[Re(R)(CO)_3(dmb)]$ (R = Me, Et, *i*Pr, benzyl) gives the same transient, at approximately 500 nm, independent of R.[4, 8]

By contrast, two transients were observed (Figure 3) for $[Re(Me)(CO)_3(dmb)]$: a long-lived one at approximately 500 nm, belonging to the $[Re(S)(CO)_3(dmb)]^{\bullet}$ radical, and a decaying one, absorbing at about 530 nm, which was assigned[8] to an unreactive ^{3}MLCT state, with some admixed ^{3}SBLCT character.[8, 22] Moreover, a weak, unresolved absorption, apparently due to both transients, extends toward long wavelengths. The assignment of the 530 nm transient to the ^{3}MLCT excited state was substantiated[8] by its characteristic TRIR spectrum and by identical absorption and emission decay lifetimes. Previously measured[8] time-resolved IR spectra have proven decisively that this state is not a precursor

0947-6539/00/0608-1388 $ 17.50+.50/0 *Chem. Eur. J.* **2000**, *6*, No. 8

to radical formation. By changing the solvent from toluene to CH_2Cl_2, the ^{3}MLCT lifetime of [Re(Me)(CO)$_3$(dmb)] is decreased from 40 to approximately 35 ns, whereas the lifetime of [Re(S)(CO)$_3$(dmb)]$^\cdot$ radicals is shortened from 7 to 5 μs.[8] All of the transients observed for both methyl and ethyl complexes were fully formed within the 7 ns laser pulse excitation, suggesting that they result from ultrafast excited-state processes.

Ultrafast dynamics of [Re(Me)(CO)$_3$(dmb)]: Figure 3, top panel, shows the time-resolved absorption spectrum of [Re(Me)(CO)$_3$(dmb)] recorded in CH_2Cl_2 at 5 ps after 400 nm laser pulse excitation. The shape and intensity of the transient absorption do not change appreciably over the next 700 ps investigated. The spectrum at 5 ps shows the features already identified[8] in the nanosecond spectra (Figure 3, bottom panel). Thus, the apparent maxima at 510 and 535 nm belong to the [Re(S)(CO)$_3$(dmb)]$^\cdot$ radical and the unreactive ^{3}MLCT state, respectively. The feature at 535 nm is much more pronounced at 5 ps than in the 10 ns spectrum, since the excited-state population is not yet diminished by decay to the ground state.

To obtain more detailed kinetic information, time profiles of the transient absorbance were measured at selected probe wavelengths. The rise of the transient absorption was followed at 480, 520, 710, and 800 nm at 100 fs intervals after excitation. Regardless of the probe wavelength, the kinetic profiles (Figure 4, ○) always followed the instrument rise function (Figure 4, broken curve). This shows that the [Re(S)(CO)$_3$(dmb)]$^\cdot$ radical and the unreactive ^{3}MLCT state are formed concurrently, by branching of the evolution of the Franck–Condon excited state. The branching time is $\leqslant$400 fs. Once formed, the transient absorbance does not change on the time scale of the experiment (usually 500 ps) (Figure 5). This behavior is consistent with the very long lifetimes of the primary photoproducts, [Re(S)(CO)$_3$(dmb)]$^\cdot$ (5 μs) and the unreactive ^{3}MLCT state (35 ns). Transient kinetics at 480 and 530 nm in CH_3CN solution were identical to those in CH_2Cl_2.

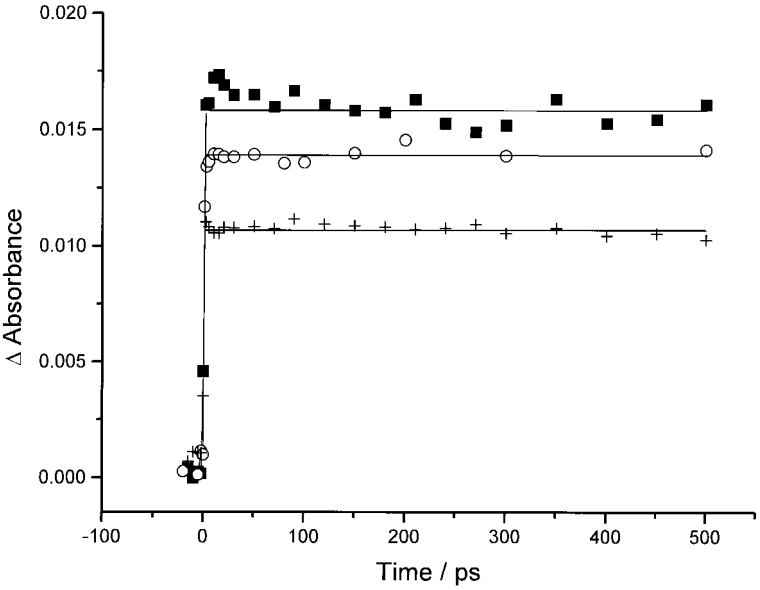

Figure 5. Kinetic profiles of the difference transient absorbance of [Re(Me)(CO)$_3$(dmb)] in CH_2Cl_2 following 400 nm laser pulse excitation; ■: probed at 530 nm with perpendicular polarization; ○: probed at 480 nm with magic angle polarization; +: probed at 800 nm with parallel polarization. The kinetic profiles measured at probe wavelengths of 435, 495, 520, 555, 665, and 710 nm were virtually identical to those shown.

Kinetic profiles of the transient absorption measured at probe wavelengths of 530 nm or higher are independent of the relative orientation of the polarization directions of the excitation and probe laser pulses, that is, parallel, perpendicular, or magic angle (54.7°). On the other hand, the kinetics probed below 530 nm—that is, in the spectral region of ground-state [Re(Me)(CO)$_3$(dmb)] absorption—are markedly polarization-dependent: perpendicular or magic angle polarization orientations give the same results as those shown in Figure 5 for longer probe wavelengths. (See, for example, the 480 nm profile probed with a magic angle orientation (Figure 5)). However, different behavior was found when probe pulses of a wavelength shorter than 530 nm were polarized parallel to the polarization direction of the excitation pulses (Figure 6). The usual sharp, instrument-limited rise of transient absorption is now followed by an additional single-exponential absorbance rise with a time

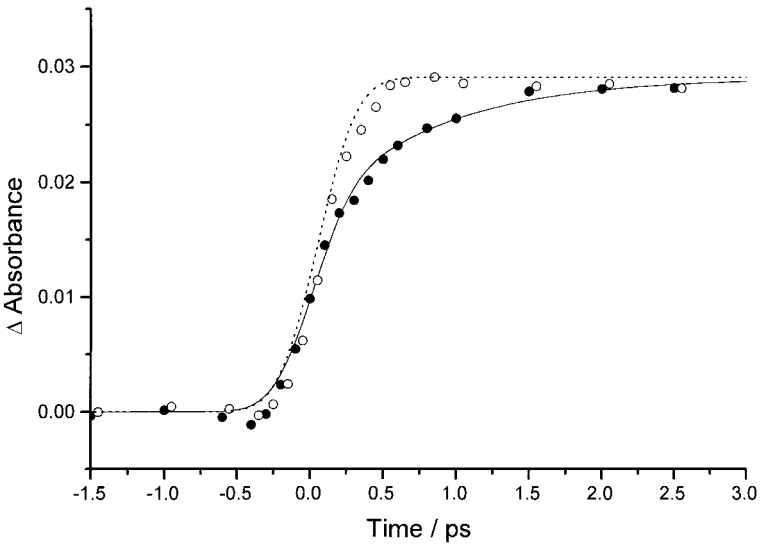

Figure 4. Kinetic profiles of the fast rise of the [Re(R)(CO)$_3$(dmb)] (R = Me, Et) transient absorption, measured in CH_2Cl_2 solution after 400 nm laser pulse excitation with a parallel orientation of the polarization directions of the excitation and probe pulses. Dotted curve: integrated instrument response function determined[32] with $[Ru(bpy)_3]^{2+}$ in CH_3CN (see Experimental section); ○: experimental data for [Re(Me)(CO)$_3$(dmb)], probed at 480 nm; ●: experimental data for [Re(Et)(CO)$_3$(dmb)], probed at 495 nm; full curve: an 800 fs exponential rise convoluted with a 600 fs gaussian instrument function.

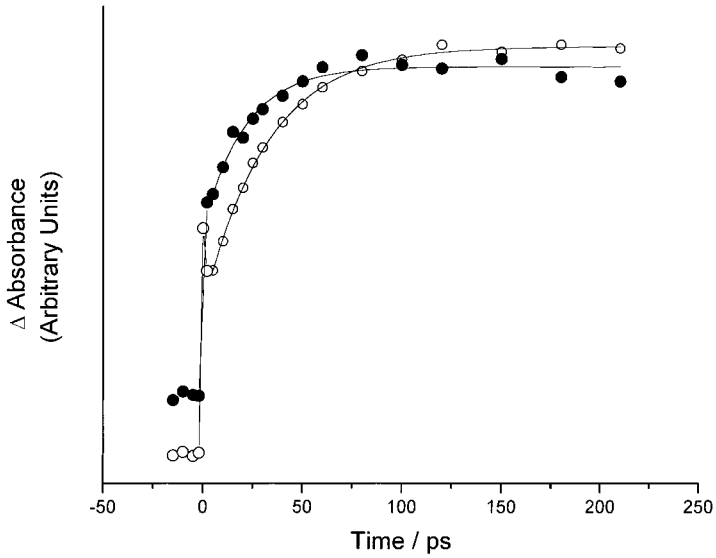

Figure 6. Kinetic profiles of the difference transient absorbance of $[Re(R)(CO)_3(dmb)]$ (R = Me, Et) in CH_2Cl_2 probed at 435 nm, obtained with a parallel orientation of polarization directions of excitation and probe pulses, after excitation at 400 nm. The two kinetic profiles are offset vertically, for clarity; ○: $[Re(Me)(CO)_3(dmb)]$; ●: $[Re(Et)(CO)_3(dmb)]$.

constant of 28 ± 4 ps. This slow rise is absent for perpendicular or magic angle orientations. This behavior can be explained by the simultaneous presence of a constant, positive transient absorption, formed within the instrumental time resolution limit, and recovery of a negative bleached ground-state absorption due to the reorientation of the unexcited ground-state $[Re(Me)(CO)_3(dmb)]$ molecules. Since the ground-state absorption of $[Re(Me)(CO)_3(dmb)]$ is strongly polarized, excitation causes a selective depletion of those $[Re(Me)(CO)_3(dmb)]$ molecules whose x axis (the C_2 symmetry axis of the Re(dmb) chromophore; Figure 1) is oriented parallel to the polarization direction of the excitation laser pulse. A probe beam polarized parallel to the excitation pulse is not absorbed by the remaining $[Re(Me)(CO)_3(dmb)]$ molecules of different orientations and hence a negative absorption signal arises immediately after excitation. Its overlap with a stronger absorption due to the photoproduced species results in a net positive transient absorption. On a longer time scale, reorientation of ground-state $[Re(Me)(CO)_3(dmb)]$ molecules replenishes the population of the parallel oriented molecules with a reorientation time constant of 28 ps. Thus, the bleached absorption recovers and the total signal increases. This effect is absent if the polarization of the probe beam is perpendicular to that of the excitation pulse, because the probe beam is absorbed by the remaining unexcited $[Re(Me)(CO)_3(dmb)]$ molecules and does not detect the orientation-dependent hole in the ground-state population. All anisotropic effects vanish when a magic angle orientation is used. Consistent with the above explanation, no polarization effects were observed at probe wavelengths longer than 530 nm, which are not absorbed by ground-state $[Re(Me)(CO)_3(dmb)]$ (Figure 5).

Ultrafast dynamics of $[Re(Et)(CO)_3(dmb)]$: Although quantum yield measurements and nanosecond spectroscopy indicate simple and efficient bond homolysis for $[Re(Et)(CO)_3(dmb)]$, a rather complex mechanism was found in the femto- and picosecond time domains. Time-resolved absorption spectra of $[Re(Et)(CO)_3(dmb)]$ in CH_2Cl_2 over a time interval of 5 – 700 ps following a 400 nm excitation are shown in Figure 2 (top panel). Surprisingly, the spectrum at 5 ps shows two apparent maxima, at approximately 505 and 530 nm. Moreover, a weak, unresolved absorption extends toward longer wavelengths, up to 700 – 800 nm (not shown). The band at 530 nm decays over the next 700 ps, leaving only the 505 nm absorption band which corresponds to $[Re(S)(CO)_3(dmb)]^{\bullet}$, identified from the nanosecond spectra (vide supra). The 530 nm feature in the 5 ps spectrum of $[Re(Et)(CO)_3(dmb)]$ is very similar to that found in the time-resolved spectra of the methyl complex over the 5 ps – 10 ns time interval; compare Figures 2 (top panel) and 3 (bottom panel). From this similarity, we conclude that the short-lived 530 nm feature belongs to the ^{3}MLCT excited state of $[Re(Et)(CO)_3(dmb)]$, which apparently has the same character as that of the methyl species. The simultaneous appearance of the 505 and 530 nm bands indicates that the radical and the ^{3}MLCT excited state are formed together, in a single, subpicosecond branching process. However, the fact that the quantum yield of radical formation from $[Re(Et)(CO)_3(dmb)]$ is unity implies that the ^{3}MLCT excited state is ultimately converted into the radical products, instead of decaying to the ground state. This provides a second, slower, photochemical pathway.[*]

To obtain more quantitative information on the processes involved in Re – Et bond homolysis, transient absorbance kinetic profiles were measured at selected probe wavelengths. Unlike the methyl complex, the rise of the transient absorption of $[Re(Et)(CO)_3(dmb)]$ is slower than the instrument rise time at all the probe wavelengths examined, that is, at 495, 710, and 800 nm (Figure 4, ●). Deconvolution of the signal rise from the Gaussian instrument response function allows us to estimate the transient rise time as 800 fs or slightly shorter, most probably in the 600 – 800 fs range. These formation dynamics are attributed to Re–Et bond homolysis via the ^{3}SBLCT state, concurrent with the population of the ^{3}MLCT state.

On a longer time scale, the transient absorbance at 495 or 530 nm decays partially, with a lifetime of 213 ± 28 ps in CH_2Cl_2 or 83 ± 15 ps in CH_3CN (Figure 7). The decay leaves a net positive transient absorption that is constant over the time interval investigated (900 ps). The decay corresponds to the conversion of the ^{3}MLCT state to the radical product, as seen in the time-resolved spectra (Figure 2). The remaining, long-lived, constant absorption is due to the $[Re(S)(CO)_3(dmb)]^{\bullet}$ radical, which absorbs weakly throughout the visible spectral region. The absorbance probed at 710 and 800 nm does not change with time on a picosecond scale after excitation. The

[*] The expected increase in the absorbance at 505 nm, concurrently with the decay of the 535 nm transient, is not apparent in the spectra shown in Figure 2 (top panel), because the two bands overlap, the weaker 505 nm band being essentially embedded in the strong, broad band of the ^{3}MLCT excited state. The transient absorption also overlaps with the region of bleached ground-state absorption, which further distorts the band shape. Moreover, the instrument signal was very low, close to the detection limit.

0947-6539/00/0608-1390 $ 17.50+.50/0 *Chem. Eur. J.* **2000**, *6*, No. 8

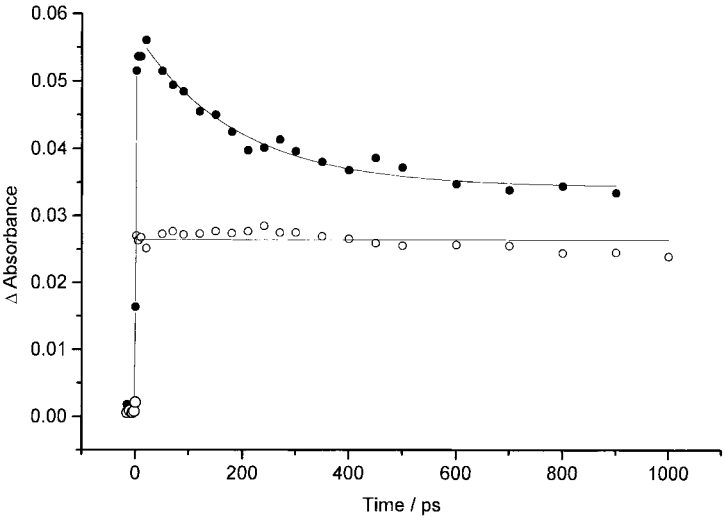

Figure 7. Kinetic profiles of the difference absorbance of [Re(Et)-$(CO)_3$(dmb)] in CH_2Cl_2 following 400 nm laser pulse excitation with parallel orientation of the polarization directions; ●: probed at 530 nm; ○: probed at 710 nm. The kinetic profile measured at 495 nm with a perpendicular or magic angle polarization orientation was the same as that shown for 530 nm. The profile obtained at 800 nm corresponded to that shown for 710 nm.

$[Re(S)(CO)_3(dmb)]^{\bullet}$ radical and the ^{3}MLCT state absorb almost equally at these wavelengths as they both possess the same chromophore: $dmb^{\bullet-}$. This is also the case for the absorptions at 430 and 450 nm; at 430 nm the absorbance time profiles are nearly constant and at 450 nm they decay with a very small amplitude. ($[M(S)(CO)_3(\alpha\text{-diimine})]^{\bullet}$ radicals can be formulated as $[M^I(S)(CO)_3(\alpha\text{-diimine}^{\bullet-})]$ (M = Mn, Re, α-diimine = bpy, phen, PyCa or dab-type ligands); this follows from EPR studies,[26, 30, 31] and is further supported[29] by the close similarity between the absorption spectra of [Re(Cl)-$(CO)_3$(dmb)]$^{\bullet-}$ and free $dmb^{\bullet-}$.)

Time profiles with a parallel polarization orientation of the excitation and probe laser pulses at 430, 450 nm and, to a much smaller extent, 495 nm show a slow rise (Figure 6) due to the reorientation of the ground-state [Re(Et)$(CO)_3$-(dmb)] molecules, analogous to that described above for the methyl complex. A reorientation time of 21 ± 3 ps was determined. This slow rise of the transient absorbance is absent from the time profiles measured with perpendicular or magic angle polarization orientations, or at longer probe wavelengths regardless of the polarization orientation.

Excited-state dynamics and mechanism of Re–alkyl bond homolysis: The ultrafast spectroscopy reported here reveals that the Re–Me bond in [Re(Me)$(CO)_3$(dmb)] is split photochemically in a single, ultrafast process whereas the homolysis of the Re–Et bond in [Re(Et)$(CO)_3$(dmb)] follows two routes: a prompt one, and a delayed pathway via an intervening excited state. Nevertheless, the primary photochemical step is the same for both complexes: regardless of the alkyl group R, the evolution of the optically prepared Franck–Condon state undergoes ultrafast branching between radical formation and population of a bound ^{3}MLCT excited state. The main difference between the ethyl and methyl complexes, which is responsible for their differing photochemistry and dynamics over the whole femto- to nanosecond time domain, lies in the behavior of this ^{3}MLCT state. It is long-lived and unreactive for [Re(Me)$(CO)_3$(dmb)], but short-lived for [Re(Et)$(CO)_3$(dmb)], ultimately decaying to radicals. The structural similarity between the two complexes and their nearly identical excited-state absorption spectra (Figures 2, 3) point to the same ^{3}MLCT character of this bound excited state for both R = Me and R = Et. Hence, a changing excited-state character cannot justify the entirely different dynamic behavior. Instead, the almost 200-fold drop in the ^{3}MLCT lifetime between the methyl and ethyl complexes is attributed to the different energy ordering of the reactive ^{3}SBLCT and bound ^{3}MLCT excited states. For R = Me, the ^{3}MLCT is the lowest excited state, whose only option is to decay to the ground state. In contrast, for the ethyl complex the ^{3}SBLCT reactive state is the lowest excited state of the molecule. Hence, the ^{3}MLCT state decays into the reactive ^{3}SBLCT state, providing a second, delayed pathway to the radical products.

Idealized qualitative potential energy curves along the Re–alkyl coordinate depict the excited-state dynamics of both complexes in Figure 8. The diagrams for [Re(Me)-$(CO)_3$(dmb)] and [Re(Et)$(CO)_3$(dmb)] are based on those calculated for [Mn(H)$(CO)_3$(H-dab)] and [Mn(Et)$(CO)_3$(H-dab)], respectively.[17, 18, 20, 21, 27] These two model molecules represent alkyl–diimine complexes with high- and low-lying

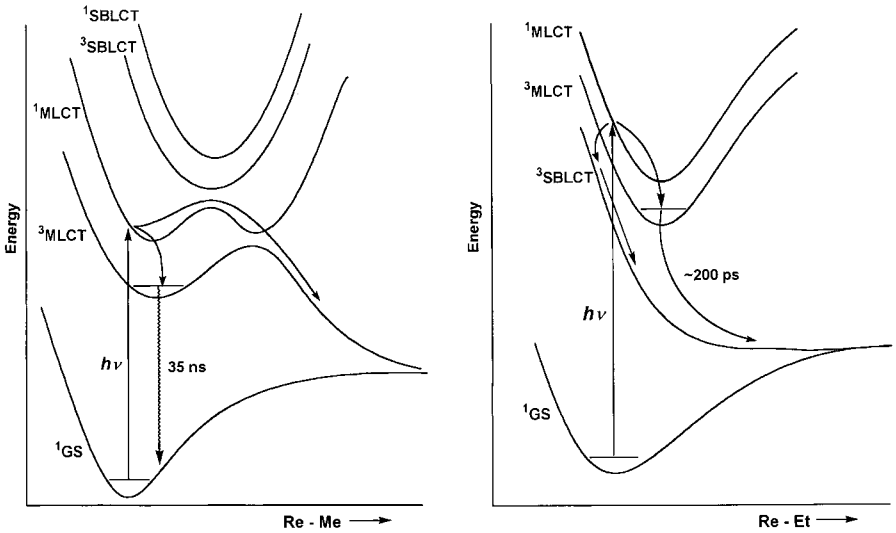

Figure 8. Qualitative excited-state potential energy curves and excited-state dynamics of [Re(R)$(CO)_3$(dmb)]. The abbreviations MLCT and SBLCT signify the predominant excited-state character at the geometry of vertical excitation. Nevertheless, even here a strong mixing of MLCT and SBLCT characters occurs.[18, 21, 22, 27, 28]

SBLCT states, respectively. Account is taken of differences in the electronic structures of Me and Et complexes,[22] the strongly mixed excited-state characters established for Re complexes,[20–22, 28] and the triplet spin multiplicity of the reactive SBLCT excited state as revealed both by calculations and FT-EPR studies.

Optical excitation of $[Re(Me)(CO)_3(dmb)]$ prepares the ^{1}MLCT Franck–Condon excited state, which, at the geometry of vertical excitation, lies below the reactive ^{3}SBLCT state and its singlet counterpart. Further along the Re–Me coordinate, the potential energy curve of the optically populated ^{1}MLCT state enters avoided crossings with the ^{1}SBLCT state and with the corresponding reactive ^{3}SBLCT triplet state. The latter avoided crossing is made possible by the spin–orbit coupling that is known to be especially strong between MLCT and SBLCT states of different spin multiplicities[25, 27, 28] and can be as large as 500 cm^{-1} in the case of Re complexes.[25, 28] These avoided crossings create a barrier on the potential energy curve of the optically populated state; beyond this barrier, the excited state acquires a dissociative ^{3}SBLCT character and evolves smoothly into the radical products, through another avoided crossing, this time with a low-lying, unreactive ^{3}MLCT state.

This model accounts for many experimental observations. The wavepacket promoted to the ^{1}MLCT Franck–Condon state either evolves along the Re–Me coordinate, over the barrier, toward the radical products, or it relaxes to the low-lying ^{3}MLCT state by prompt intersystem crossing. This branching occurs within 400 fs after excitation. The efficiency of the reactive channel population determines the photochemical quantum yield, which is 0.4 at 293 K.[8] Hence the branching ratio at 293 K is $0.4/0.6 = 0.67$. Clear evidence for the presence of an energy barrier on the reactive pathway is provided by an Arrhenius-type decrease of the quantum yield of radical formation with temperature (apparent activation energy 1560 cm^{-1}).[8] The bound ^{3}MLCT state lies deep below the reactive state and acts as an excitation energy trap. Once populated, it undergoes only nonradiative and radiative decay to the ground state. In accordance with this mechanistic model, no radical formation was observed in a low-temperature glass at 123 K, whereas the unreactive ^{3}MLCT state is still amply populated, making $[Re(Me)(CO)_3(dmb)]$ strongly emissive at low temperatures.[8, 26]

For $[Re(Et)(CO)_3(dmb)]$, the dissociative ^{3}SBLCT state is the lowest excited state of the molecule everywhere along the Re–Et reaction coordinate. Strong coupling and intersystem crossing between ^{1}MLCT, ^{3}SBLCT, and ^{3}MLCT states occurs in the region of vertical excitation, very early on the reaction coordinate (Figure 8). Following optical excitation into the ^{1}MLCT excited state, branching takes place between population of the reactive ^{3}SBLCT and of the bound ^{3}MLCT excited states. Once the dissociative ^{3}SBLCT state is populated, Re–Et bond homolysis proceeds and radicals are formed. The branching time (600–800 fs) is somewhat longer than in the case of the methyl complex ($\leq$400 fs), presumably because of the difference in the ordering and potential energy curve shapes of the relevant states. This now requires the ^{1}MLCT$\rightarrow$^{3}SBLCT intersystem crossing to follow a tunneling mechanism, which resembles Marcus inverted behavior (see Figure 8). The bound ^{3}MLCT state, populated concurrently with radical formation, is not inherently reactive. However, since the dissociative ^{3}SBLCT potential energy surface lies immediately below the ^{3}MLCT state, the latter eventually decays onto the reactive ^{3}SBLCT surface, on which radicals are formed. The bound ^{3}MLCT state does not act as a trapping state per se in the ethyl complex, since its population does not prevent, but only delays, the Re–Et homolysis to the radicals. The experimentally measured lifetime of the excited state (213 ps in CH_2Cl_2; 83 ps in CH_3CN) is determined by the rate of conversion of the ^{3}MLCT to the ^{3}SBLCT state. The ordering of the excited states of $[Re(Et)(CO)_3(dmb)]$ does not give rise to any energy barriers. Accordingly, the photochemical quantum yield of Re–Et bond homolysis is independent of the temperature. Radicals are formed from $[Re(Et)(CO)_3(dmb)]$, even in a low-temperature glass at 123 K, but no emission occurs because of the absence of any low-lying trapping state.[8, 26] The great difference in the photochemical and photophysical behavior of the methyl and ethyl complexes in low-temperature glasses strongly supports the mechanistic models developed above.

The proposed difference in ordering of the Franck–Condon ^{1}MLCT, reactive ^{3}SBLCT, and bound ^{3}MLCT states in $[Re(Me)(CO)_3(dmb)]$ and $[Re(Et)(CO)_3(dmb)]$ is fully in line with the results of recent CASSCF/MR-CCI calculations on model $[Mn(R)(CO)_3(H\text{-}dab)]$ complexes (R = H, Me, Et,[22] which have revealed that, on going from Me to Et, the ^{1}SBLCT state decreases in energy relative to ^{1}MLCT while the energy difference between corresponding triplets diminishes. These differences were attributed to the fact that Mn–Et is a weaker and less polar bond than Mn–Me. In another theoretical study, the lowest triplet excited state of $[Mn(Et)(CO)_3(H\text{-}dab)]$ was indeed calculated to be dissociative along the Mn–Et coordinate whereas the upper one is bound.[27] The situation is reversed for $[Mn(H)(CO)_3(H\text{-}dab)]$.[17, 18, 20, 21, 27] Again in agreement with present experimental data, the correlation diagram calculated for $[Mn(Et)(CO)_3(H\text{-}dab)]$ reveals a smooth, barrierless correlation between the lowest excited triplet state and the radical products.[20] However, a state crossing, which creates an energy barrier, appears in correlation diagrams of $[Mn(Me)(CO)_3(H\text{-}dab)]$ and $[Mn(H)(CO)_3(H\text{-}dab)]$.[20]

However well the excited-state potential energy surfaces account for the experimentally determined excited-state dynamics and mechanism of the Re–alkyl bond homolysis in $[Re(R)(CO)_3(dmb)]$, some issues remain open. Firstly, it is the role of the large spin–orbit coupling of the Re atoms which will not only guarantee fast intersystem crossing, but also lift the degeneracy of triplet excited states by up to 1200 cm^{-1}.[25] Individual spin sublevels of the ^{3}SBLCT can differ in reactivity, as was indicated by FT-EPR experiments on $[Re(R)(CO)_3(dmb)]$.[8, 23, 24] Secondly, the nature of the diimine ligand plays a very important role. Unlike $[Re(Et)(CO)_3(dmb)]$, the ^{3}SBLCT state in $[Re(R)(CO)_3(i\text{Pr-}dab)]$ (R = Et, benzyl) appears to be bound in hydrocarbon solutions, where radicals are produced on a time scale of tens to hundreds of nanoseconds.[5–7] Thirdly, the solvent has a large influence, since the Re–R homolysis in $[Re(R)(CO)_3(i\text{Pr-}dab)]$ is more than 10^5 times faster in THF or

0947-6539/00/0608-1392 $ 17.50+.50/0 *Chem. Eur. J.* **2000**, *6*, No. 8

CH_3CN than in hydrocarbon solvents.[6, 7] The energy ordering and shape of potential energy curves of excited states of [Re(R)(CO)$_3$(α-diimine)] complexes are clearly very sensitive to variations in the alkyl and α-diimine ligands as well as to changes of the medium in a way which warrants further investigation.

Conclusions

The kinetics, mechanism, and quantum yield of Re–alkyl bond homolysis in alkyl–diimine complexes [Re(R)(CO)$_3$(dmb)] (R = Me, Et) are strongly dependent on the relative positions of the Franck–Condon ^{1}MLCT, reactive ^{3}SBLCT and bound ^{3}MLCT excited states, both in the region of vertical excitation and along the Re–alkyl reaction coordinate. The degree of coupling between these states also has a very important influence.

The primary photochemical step is similar for both complexes (R = Me or Et): branching of the evolution of the optically prepared ^{1}MLCT state between homolysis via the reactive ^{3}SBLCT state and population of a bound, inherently unreactive, ^{3}MLCT excited state. Provided that the reactive ^{3}SBLCT excited state lies above the Franck–Condon state (R = Me), an energy barrier can develop on the reactive pathway, leading to temperature-dependent photochemistry.

Later stages of the excited-state dynamics of [Re(R)(CO)$_3$(dmb)] (R = Me, Et) depend on the relative energy position of the two lowest triplet states, namely the reactive ^{3}SBLCT and bound ^{3}MLCT excited states. If the bound ^{3}MLCT state is the lowest excited state of the molecule, it acts as an excitation energy trap, as was found for [Re(Me)(CO)$_3$(dmb)]. In this situation the quantum yield is determined by the efficiency of the primary step, that is, of the branching between population of reactive and relaxation channels from the optically prepared Franck–Condon state. Such a molecule is expected to show emission, especially at low temperatures. However, if the bound state lies above the reactive one, as for [Re(Et)(CO)$_3$(dmb)], its population provides another, delayed, reactive pathway and the homolysis quantum yield is close to unity, regardless of the initial branching ratio. The organometallic molecule is then not emissive, but remains highly photoreactive even at low temperatures.

Branching of the Franck–Condon state between reactive and trapping excited states appears to be a general feature of the early excited-state dynamics of photoreactive organometallic complexes, observed,[32, 33] for example, for [Cr(CO)$_4$(bpy)] or [Cp*M(CO)$_2$] (M = Ir, Rh).

Experimental Section

The complexes [Re(R)(CO)$_3$(dmb)] (R = Me, Et) were prepared and characterized according to a literature procedure.[26] Spectroscopic-grade solvents were obtained from Aldrich and degassed by bubbling with high-purity argon.

The quantum yield of the photoreaction of [Re(Et)(CO)$_3$(dmb)] was measured in toluene by a procedure described previously.[8] Samples were irradiated with a 488 nm Ar^+ laser line. Typical incident light intensities were in the range $(8–13) \times 10^{-9}$ einstein s^{-1}. Several experiments afforded quantum yield values in the range 1.1–1.2 which, given the difficulties with measurements of high quantum yields, approximates to 1. The quantum yield is independent of temperature in the range examined (253–293 K). Previous measurements[26] in CH_2Cl_2 gave a value of 1.

Nanosecond measurements were performed on an instrument described previously. [8] Sample solutions were excited at 355 nm by 7 ns laser pulses (FWHM) obtained by frequency tripling the 1064 nm output of a Spectra Physics GCR-3 Nd:YAG laser operating at 10 Hz. Transient absorption was recorded for a perpendicular beam geometry with an EG & G FX-504 high-power Xe lamp. Transient spectra were obtained with an Acton Spectropro 150 s imaging spectrograph and an ICCD-576EMG/RB detector. The sample solution, absorbance 0.6, was flowed through a 1 cm pathlength cell.

Ultrafast spectroscopic experiments were carried out on flowing, degassed solutions whose absorbance at the excitation wavelength was in the range 0.6–1.0. The solution was kept in the dark during measurements and continuously degassed with argon. Measurements were complicated by sample photodecomposition on the cell surface which reduced the signal-to-noise ratio and severely limited the accuracy of lifetime determinations. To minimize this effect, the excitation laser beam had to be slightly defocused and/or its intensity diminished with a gray filter, optical density 0.5–0.9. Net sample photodecomposition during the measurements was found by UV/Vis absorption spectroscopy to be negligible. The pump-probe, femtosecond, time-resolved spectroscopy setup has been described in great detail elsewhere.[32, 34–36] The sample was excited by means of the 400 nm second harmonics of a Spectra Physics Tsunami titanium–sapphire regenerative amplifier operating at a repetition rate of approximately 1 kHz, producing pulses of approximately 250 fs (FWHM). Pulse energy was in the range 1–3 μJ. The white light continuum probe beam was generated by passing the Ti:sapphire fundamental through a cell containing flowing D_2O. The delay between the excitation and probe pulses was controlled by an optical delay line. Diode array detection involved dividing the probe pulse into two parts, of which one was sent through the sample before dispersing it onto a 512-pixel diode array, and the other was dispersed directly onto a reference array, bypassing the sample. Alternate laser excitation pulses were blocked by means of a mechanical chopper. Data were collected from these diode arrays over 20 s periods for each time delay. To reduce systematic errors due to sample degradation, long-term laser power changes, and suchlike, measurements at individual delay times were repeated 10 times in a random order. The data were processed to give difference absorption spectra (that is, the spectrum after excitation minus the spectrum before excitation). Kinetic profiles at single wavelengths were measured by means of probe pulses obtained by selecting a portion of the white light continuum with 10 nm bandpass interference filters. Kinetic traces at 800 nm were monitored by using the fundamental pulses of the regenerative amplifier as the probe beam. The excitation beam was chopped mechanically at a frequency of approximately 200 Hz. The intensities of the sample and reference probe beams were monitored with two photodiodes. An analogue ratio of the photodiode signals was fed into a lock-in amplifier. Signals were accumulated for 5 s at each delay time and the whole measurement was repeated at least 10 times, again in a random order of delay times. The data were processed to give the difference between the sample absorbance measured with and without laser excitation (ΔAbsorbance) as a function of the delay time.

The time resolution of the instrument was estimated[32] with $[Ru(bpy)_3]^{2+}$ in acetonitrile solution. The rise in transient absorption of $[Ru(bpy)_3]^{2+}$ (Figure 4) was assumed to be coincident with the integrated instrument response function. The instrument rise time was estimated to be 600 fs or better. Computer simulations using a 600 fs gaussian response function convoluted with various exponentially rising signals indicate that rise times of 400 fs and longer can be detected confidently with the current experimental setup.

Experimental kinetic profiles were fitted with Microcal Origin version 5.0 software. The femtosecond rise observed for [Re(Et)(CO)$_3$(dmb)] was fitted to a function of the convoluted exponential rise and gaussian instrument response function of a fixed 600 fs FWHM. Fastfit software (University of York, UK) was used. Alternatively, the experimental data were compared with results of computer simulations of various formation kinetics convoluted with the instrument response function, using purpose-written software.

Acknowledgements

We thank Mike Towrie and Tony Parker of the Rutherford Appleton Laboratory for their technical assistance and stimulating discussions. Davina Liard is thanked for her help in recording the ultrafast diode array spectra. Many stimulating and enlightening discussions with Derk Stufkens (University of Amsterdam) and Chantal Daniel (CNRS Strasbourg) are gratefully acknowledged. We also thank EPSRC and Queen Mary and Westfield College (University of London) for funding. This work was undertaken as part of the European collaborative COST projects D4/0001/94 and D14/0001/99.

[1] D. J. Stufkens, M. P. Aarnts, B. D. Rossenaar, A. Vlček, Jr., *Pure Appl. Chem.* **1997**, *69*, 831 – 835.
[2] D. J. Stufkens, M. P. Aarnts, J. Nijhoff, B. D. Rossenaar, A. Vlček, Jr., *Coord. Chem. Rev.* **1998**, *171*, 93 – 105.
[3] D. J. Stufkens, A. Vlček, Jr., *Coord. Chem. Rev.* **1998**, *177*, 127 – 179.
[4] L. A. Lucia, R. D. Burton, K. S. Schanze, *Inorg. Chim. Acta* **1993**, *208*, 103 – 106.
[5] B. D. Rossenaar, C. J. Kleverlaan, D. J. Stufkens, A. Oskam, *J. Chem. Soc. Chem. Commun.* **1994**, 63 – 64.
[6] B. D. Rossenaar, M. W. George, F. P. A. Johnson, D. J. Stufkens, J. J. Turner, A. Vlček, Jr., *J. Am. Chem. Soc.* **1995**, *117*, 11582 – 11583.
[7] B. D. Rossenaar, C. J. Kleverlaan, M. C. E. van de Ven, D. J. Stufkens, A. Vlček, Jr., *Chem. Eur. J.* **1996**, *2*, 228 – 237.
[8] C. J. Kleverlaan, D. J. Stufkens, I. P. Clark, M. W. George, J. J. Turner, D. M. Martino, H. van Willigen, A. Vlček, Jr., *J. Am. Chem. Soc.* **1998**, *120*, 10871 – 10879.
[9] J. E. Hux, R. J. Puddephatt, *J. Organomet. Chem.* **1992**, *437*, 251 – 263.
[10] S. Hasenzahl, H.-D. Hausen, W. Kaim, *Chem. Eur. J.* **1995**, *1*, 95 – 99.
[11] W. Kaim, A. Klein, S. Hasenzahl, H. Stoll, S. Záliš, J. Fiedler, *Organometallics* **1998**, *17*, 237 – 247.
[12] E. Wissing, E. Rijnberg, P. A. van der Schaaf, K. van Gorp, J. Boersma, G. van Koten, *Organometallics* **1994**, *13*, 2609 – 2615.
[13] B. D. Rossenaar, E. Lindsay, D. J. Stufkens, A. Vlček, Jr., *Inorg. Chim. Acta* **1996**, *250*, 5 – 14.
[14] J. W. M. van Outersterp, M. T. G. Oostenbrink, H. A. Nieuwenhuis, D. J. Stufkens, F. Hartl, *Inorg. Chem.* **1995**, *34*, 6312 – 6318.
[15] J. Nijhoff, M. J. Bakker, F. Hartl, D. J. Stufkens, W.-F. Fu, R. van Eldik, *Inorg. Chem.* **1998**, *37*, 661 – 668.
[16] M. Kaupp, H. Stoll, H. Preuss, W. Kaim, T. Stahl, G. van Koten, E. Wissing, W. J. J. Smeets, A. L. Spek, *J. Am. Chem. Soc.* **1991**, *113*, 5606 – 5618.
[17] K. Finger, C. Daniel, *J. Chem. Soc. Chem. Commun.* **1995**, 1427 – 1428.
[18] K. Finger, C. Daniel, *J. Am. Chem. Soc.* **1995**, *117*, 12322 – 12327.
[19] K. Finger, C. Daniel, P. Saalfrank, B. Schmidt, *J. Phys. Chem.* **1996**, *100*, 3368 – 3376.
[20] D. Guillaumont, K. Finger, M. R. Hachey, C. Daniel, *Coord. Chem. Rev.* **1998**, *171*, 439 – 459.
[21] D. Guillaumont, C. Daniel, *Coord. Chem. Rev.* **1998**, *177*, 181 – 199.
[22] D. Guillaumont, M. P. Wilms, C. Daniel, D. J. Stufkens, *Inorg. Chem.* **1998**, *37*, 5816.
[23] C. J. Kleverlaan, D. M. Martino, H. van Willigen, D. J. Stufkens, A. Oskam, *J. Phys. Chem.* **1996**, *100*, 18607 – 18611.
[24] C. J. Kleverlaan, D. M. Martino, J. van Slageren, H. van Willigen, D. J. Stufkens, A. Oskam, *Appl. Magn. Reson.* **1998**, *15*, 203 – 214.
[25] C. Daniel, D. Guillaumont, C. Ribbing, B. Minaev, *J. Phys. Chem. A* **1999**, *103*, 5766 – 5772.
[26] C. J. Kleverlaan, D. J. Stufkens, *Inorg. Chim. Acta* **1999**, *284*, 61 – 70.
[27] D. Guillaumont, C. Daniel, *J. Am. Chem. Soc.* **1999**, *121*, 11733 – 11743.
[28] D. Guillaumont, C. Daniel, unpublished results.
[29] B. D. Rossenaar, D. J. Stufkens, A. Vlček, Jr., *Inorg. Chim. Acta* **1996**, *247*, 247 – 255.
[30] R. R. Andrea, W. G. J. de Lange, T. van der Graaf, M. Rijkhoff, D. J. Stufkens, A. Oskam, *Organometallics* **1988**, *7*, 1100 – 1106.
[31] A. Klein, C. Vogler, W. Kaim, *Organometallics* **1996**, *15*, 236 – 244.
[32] I. R. Farrell, P. Matousek, A. Vlček, Jr., *J. Am. Chem. Soc.* **1999**, *121*, 5296 – 5301.
[33] S. E. Bromberg, T. Lian, R. G. Bergman, C. B. Harris, *J. Am. Chem. Soc.* **1996**, *118*, 2069 – 2072.
[34] P. Matousek, A. W. Parker, P. F. Taday, W. T. Toner, M. Towrie, *Opt. Commun.* **1996**, *127*, 307 – 312.
[35] M. Towrie, A. W. Parker, W. Shaikh, P. Matousek, *Meas. Sci. Technol.* **1998**, *9*, 816 – 823.
[36] M. Towrie, P. Matousek, A. W. Parker, S. Jackson, R. H. Bisby, *Rutherford Appleton Laboratory Report* **1997/1998**, 183.

Received: June 10, 1999 [F1841]

  0947-6539/00/0608-1394 $ 17.50+.50/0